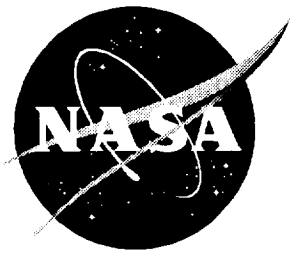

NASA Technical Memorandum 4658

High-Precision Buffer Circuit for Suppression of Regenerative Oscillation

John S. Tripp, David A. Hare, and Ping Tcheng

May 1995

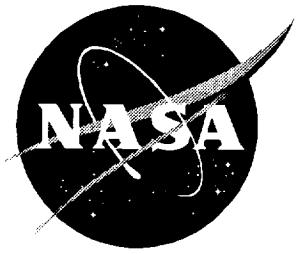

NASA Technical Memorandum 4658

High-Precision Buffer Circuit for Suppression of Regenerative Oscillation

John S. Tripp, David A. Hare, and Ping Tcheng
Langley Research Center • Hampton, Virginia

May 1995

Available electronically at the following URL address: http://techreports.larc.nasa.gov/ltrs/ltrs.html

Printed copies available from the following:

NASA Center for AeroSpace Information
800 Elkridge Landing Road
Linthicum Heights, MD 21090-2934
(301) 621-0390

National Technical Information Service (NTIS)
5285 Port Royal Road
Springfield, VA 22161-2171
(703) 487-4650

Symbols

AOA	angle of attack, deg
b_k	transfer function denominator polynomial coefficients, $k = 1, 2$
C_A	snubber circuit capacitance, F
C_F	feedback network roll-off capacitance, F
C_L	load capacitance, F
D	discriminant
DAS	data acquisition system
DC	denotes constant voltage
DVM	digital voltmeter
E_i	Laplace transform of network input voltage
E_o	Laplace transform of network output voltage
FS	full scale
K	operational amplifier open-loop gain, V/V
p_k	poles of transfer function T_S, $k = 1, 2$
ppm	parts per million
R_A	snubber network resistance, Ω
R_S	operational amplifier open-loop source resistance, Ω
R_1, R_F	filter network resistance, Ω
RC	resistance capacitance
RTO	referred to output
rms	root mean square
s	Laplace transform operator
T	transfer function of compensated filter
T_B	transfer function of uncompensated unity-gain buffer
T_C	transfer function of compensated unity-gain buffer
T_S	transfer function of snubber/output circuit
T_U	transfer function of uncompensated filter
x	variable
τ_A	time constant of snubber circuit, sec
τ_F	time constant of uncompensated filter output circuit, sec
τ_L	time constant of uncompensated unity-gain buffer circuit, sec
τ_1, τ_2	time constants of operational amplifier, sec
ω_0	frequency of regenerative oscillation, rad/sec

Introduction

Precision servo accelerometers are employed at the Langley Research Center for measurement of wind tunnel model attitude or angle of attack (AOA) to an accuracy of ±0.01° (ref. 1). These sensors, whose output levels must be measured to microvolt accuracy, require signal conditioning electronics with heavy low-pass filtering and highly accurate DC gain. Moreover, the signal conditioning electronics may not contribute additional errors to the analog accelerometer output voltages by more than ±10 μV DC offset and ±20 μV noise in order to maintain an AOA measurement accuracy of ±0.01°. The combined requirements for low noise, low DC offset, high isolation, four-pole Bessel response, and greater than unity gain require the use of precision chopper-stabilized operational amplifiers in the active low-pass filter circuit supplying the prime filtered AOA analog output to an integrating digital voltmeter (DVM) via the analog signal distribution system of the wind tunnel. Additional unity-gain buffered outputs for the prime filtered and unfiltered dynamic AOA signals are required for supplementary inputs to the facility data acquisition system (DAS) and any user-furnished instrumentation. The capacitive loads due to cables and the facility signal distribution patchboard were found to cause regenerative oscillations at approximately 400 kHz at a 0.5-V amplitude in the output stages of the prototype signal conditioner. The output buffer circuits required regenerative oscillation suppression while maintaining low output impedance, low noise, and low DC offset at microvolt levels with ample design tolerances. A technique employing a series load resistor occasionally used to damp oscillation in certain analog circuits (ref. 2) was not acceptable for this application because of requirements for low output impedance, high output isolation, and high common mode rejection at the measuring instrument. A known oscillation suppression circuit (ref. 3) using a series resistor-capacitor pair inserted in parallel with the load, colloquially termed a "snubber" circuit, which meets the design requirements, was employed. A design procedure employing feedback control compensation theory was developed to investigate stability, to compute phase margin, and to select component values for this circuit. Practical design formulas are provided.

The accuracy requirements of AOA measurement impose the following performance specifications for the active filter and buffer circuits:

1. Provide high isolation between AOA signal conditioner and facility analog signal distribution and DAS input stages
2. Provide low output impedance: <1 mΩ below 10 Hz
3. Maintain low signal conditioner output noise level: <20 μV rms referred to output (RTO)
4. Maintain low signal conditioner output DC offset level: <20 μV RTO
5. Maintain high common mode rejection between buffer output and facility DAS inputs: >120 dB
6. Maintain DC linearity and gain accuracy: <0.02 percent FS
7. Accommodate moderate input impedance at the driven DAS input stage: ≥10 kΩ with gain error less than ±0.005 percent
8. Drive capacitive cable and analog distribution system loads: < 100 nF
9. Suppress regenerative oscillation

Circuit Description

Figure 1 illustrates the block diagram of the AOA signal conditioner containing a four-pole, active, low-pass Bessel filter, implemented by using two cascaded two-pole Sallen-Key (ref. 4) noninverting stages and two unity-gain buffered output stages. The filter output stage, which also serves as a buffer, furnishes the prime static AOA output to the facility DVM/DAS. The unity-gain buffers furnish an isolated static AOA output and an unfiltered dynamic AOA output. All active stages and buffers employ precision advanced LinCMOS[1] ultra-low offset chopper-stabilized operational amplifiers, type 2652A.

Figure 2 depicts the output stage of the active Bessel filter, which serves as the buffer circuit for the prime AOA output. The operational amplifier is modeled within the first dashed-line box, showing the input differential stage, open-loop gain $K \geq 10^7$, the transfer function with time constants $\tau_1 = 1/20\pi$ sec, and $\tau_2 = 1/10^7\pi$ sec, and equivalent output resistance $R_S = 50\ \Omega$. Shown in the third dashed-line box is the gain and noise roll-off network. Gain resistors R_F and R_1 furnish a gain of 11, and capacitor C_F, installed in parallel with feedback gain resistor R_F, limits output noise to 20 μV rms. Figure 3 illustrates the unity-gain buffer circuit, provided for the dynamic AOA output and the secondary static AOA output, in which the gain and noise roll-off network is omitted.

The uncompensated filter output stage experienced regenerative oscillation for total cable and patch-panel capacitive loads exceeding 3 nF, with significant DC offset due to nonlinear effects. Table 1 presents amplitude and frequency of oscillation and the associated DC

[1] Advanced LinCMOS is a trademark of Texas Instruments, Inc.

Table 1. Oscillation Frequency and Amplitude Versus Load Capacitance

Load capacitance, nF	Frequency, kHz	Amplitude (peak-to-peak), V	DC offset, mV
<2.9	No oscillation		0.013
2.9	413	1.09	390
5	313	1.19	746
10	243	0.91	668

offset, for capacitive loads from 0 to 10 nF observed during laboratory tests. From the experimental values, the phase shift of the open-loop system would be −180° at oscillation frequencies near 300 kHz or 2×10^6 rad/sec. Consequently, phase-lead compensation is needed to stabilize the closed-loop system.

Manufacturer's data sheets (ref. 5) for the chopper-stabilized operational amplifier used indicate that its phase margin decreases from 50° to 12° as the load capacitance increases from 0 to 1 nF and the open-loop transfer function contains real poles at approximately 10 Hz and 5 MHz with an open-loop gain of 10^7. Gain-phase analysis, as described subsequently, shows that the buffer circuit is unstable when terminated with capacitive loads greater than 3 nF. The 3-nF threshold value was verified experimentally, as shown in table 1.

A commonly used stabilization technique (ref. 6) employs a lead-lag network, configured identically to the gain and noise roll-off network composed of components R_F, C_F, and R_1 shown in the third dashed-line box of figure 2. This network introduces sufficient phase lead to produce adequate phase margin for stability. However, because the value of capacitor C_F required for noise suppression is 1 μF and the value of C_F required for stabilization is 10 pF, this network cannot perform both noise suppression and stabilization functions simultaneously. Two additional buffered lead-lag stages could be cascaded with the filter output to provide stabilized prime and secondary static AOA outputs, and another buffered lead-lag stage could be employed for the unfiltered dynamic AOA output. However, this would impose unwanted gains of 11, and it would also worsen high-frequency noise rejection. Therefore, the selected stabilization technique employs a series resistance-capacitance (RC) snubber network installed in parallel with the output load as shown in the second dashed-line rectangle in figures 2 and 3. This circuit is analyzed through the use of gain-phase analysis as described in the following paragraphs.

Stability Analysis

Uncompensated Unity-Gain Buffer Circuit

The uncompensated unity-gain buffer circuit is shown in figure 3, which includes the equivalent operational amplifier transfer function, open-loop gain K, open-loop output resistance R_S, and load capacitance C_L. By means of nodal equations, the open-loop transfer function between output E_o and input E_i is obtained in Laplace transform notation as

$$T_B(s) = \frac{E_o(s)}{E_i(s)} = \frac{K}{(1+\tau_1 s)(1+\tau_2 s)(1+\tau_L s)} \quad (1)$$

where

$$\tau_1 = \frac{1}{20\pi}$$

$$\tau_2 = \frac{1}{10^7\pi}$$

$$\tau_L = R_S C_L$$

and s is the Laplace transform operator.

The gain-phase plot of $T_B(s)$ appears in figure 4. Note that the phase shift at unity gain is −225° at 4×10^7 rad/sec; this indicates unstable operation with a −45° phase margin. Figure 5 illustrates the gain-phase plot of the load circuit alone, consisting of open-loop source resistance R_S and load capacitance C_L, whose transfer function equals $1/(1+\tau_L s)$. Note that the phase shift approaches −90° for frequencies above 10^7 rad/sec, which when combined with that of the operational amplifier transfer function, produces the total −225° phase shift at unity gain seen in figure 4.

Snubber Circuit

The intent is to place a compensation network in cascade with the output of the operational amplifier which will introduce sufficient phase lead in the region near oscillation frequency ω_0 to produce adequate phase margin. The effect of the snubber circuit on the unity-gain buffer can be readily seen by analysis of the RC network consisting of the snubber network in parallel with the capacitive load shown in figure 3.

Transfer function. The transfer function of this network, composed of open-loop source resistance R_S, snubber network $R_A C_A$, and load capacitor C_L, is found, by using nodal equations, to be

$$T_S(s) = \frac{1 + \tau_A s}{1 + b_1 s + b_2 s^2} \tag{2}$$

where

$$\left.\begin{aligned} \tau_A &= R_A C_A \\ b_1 &= R_A C_A + R_S C_L + R_S C_A \\ b_2 &= R_A R_S C_A C_L \end{aligned}\right\} \tag{3}$$

Circuit analysis. From network theory, the poles and zeros of any RC network alternate along the negative real axis of the complex plane (ref. 7). Indeed, the discriminant of the denominator of equation (2) is given by

$$D = b_1^2 - 4b_2 \tag{4}$$

Combine equations (3) and (4) and simplify to obtain

$$D = (R_A C_A - R_S C_L + R_S C_A)^2 + 4R_S^2 C_L C_A > 0 \tag{5}$$

showing that the poles of equation (2) are real.

Selecting values of R_A and C_A such that the zero of $T_S(s)$ is near ω_0 and the poles are widely separated about ω_0 ensures significantly reduced phase lag in a region about ω_0. Set $\tau_A = 1/\omega_0$ to place the zero of equation (2) close to ω_0, this, in turn, fixes the value of b_2 and leaves only a single free parameter, say C_A. The poles of equation (2) are given by

$$p_1, p_2 = -\frac{b_1}{2b_2}\left[1 \pm \left(1 - \frac{4b_2}{b_1^2}\right)^{1/2}\right] \tag{6}$$

Now it can be shown that the square-root function is well approximated by the following:

$$(1 + x)^{1/2} \approx 1 + \frac{1}{2}x \tag{7}$$

for $|x| < 0.1$. Let $x = 4b_2/b_1^2$ and combine equations (6) and (7) to obtain poles p_1 and p_2 as

$$p_1 \approx -\frac{1}{b_1} \tag{8}$$

and

$$p_2 \approx -\frac{b_1}{b_2} \tag{9}$$

In order to provide a wide region of minimum phase shift about ω_0 for the compensation circuit, a parametric study was conducted to determine proper pole-zero placement. It showed that poles p_1 and p_2 should be placed approximately two decades on either side of ω_0. Therefore, R_A and C_A should be selected to satisfy the following two inequalities:

$$|p_1| \le 0.01\omega_0 \tag{10}$$

and

$$|p_2| \ge 100\omega_0 \tag{11}$$

Note from inequalities (10) and (11) that the square-root approximation (7) used in equation (6) is accurate for this pole placement, since the condition $|x| < 0.1$ is satisfied thusly:

$$|x| = \frac{4b_2}{b_1^2} \approx \frac{4|p_1|}{|p_2|} \le 4 \times 10^{-4} < 0.1 \tag{12}$$

Hence approximations (8) and (9) are accurate.

Design procedure. Combine equations (3) and (8) and inequality (10) to obtain

$$|p_1| \approx \frac{1}{b_1} = \frac{1}{(1/\omega_0) + R_S C_L + R_S C_A} \le \frac{\omega_0}{100} \tag{13}$$

therefore, C_A must satisfy

$$C_A \ge \frac{99}{\omega_0 R_S} - C_L \tag{14}$$

Similarly, equations (3) and (9) and inequality (11) are combined to obtain

$$|p_2| \approx \frac{b_1}{b_2} = \omega_0 + \frac{1}{R_S C_L} + \frac{1}{R_A C_L} \ge 100\omega_0 \tag{15}$$

from which it follows that R_A must satisfy

$$R_A \le \frac{R_S}{99\omega_0 C_L R_S - 1} \tag{16}$$

Compensated Unity-Gain Buffer

The open-loop transfer function of the snubber compensator cascaded with the unity-gain buffer, as shown in figure 3, is given by the product of equation (2) with the gain and poles of the operational amplifier thusly:

$$T_C(s) = \frac{K(1 + \tau_A s)}{(1 + \tau_1 s)(1 + \tau_2 s)\left(1 + b_1 s + b_2 s^2\right)} \tag{17}$$

Application of Design Equations

Snubber circuit component values are now selected for the precision buffer circuit, where $R_S = 50\ \Omega$, $C_L = 5$ nF, and $\omega_0 = 2 \times 10^6$ rad/sec. For these values, conditions (14) and (16) predict limiting values of

$C_A \geq 1\ \mu F$ and $R_A \leq 1\ \Omega$, respectively. Gain-phase analysis of the unity-gain buffer compensated with these limiting component values, described by equation (17), indicates that the closed-loop circuit is stable with a 62° phase margin at 1.15×10^7 rad/sec.

The limiting component values are used as initial approximations for the selection of the snubber compensation circuit parameters. Parametric studies are then necessary to trim the initial approximations to the values required to attain the desirable 45° phase margin (ref. 6). Figure 6 illustrates the gain-phase plot of transfer function $T_S(s)$ of the compensated load represented by equation (2) with the values C_A = 220 nF and R_A = 1 Ω. These values, obtained from the parametric studies, yield a closed-loop response with a 45.5° phase margin at 1.20×10^7 rad/sec. Note in figure 6 that the phase shift of the transfer function of the compensated load $T_S(s)$ is approximately −20° in the region between 10^7 and 10^8 rad/sec because of the phase lead introduced by the zero at $1/\tau_A$ compared with a −90° phase shift in the same region of the transfer function of the uncompensated load shown in figure 5. Figure 7 illustrates the gain-phase plot of the compensated unity-gain buffer terminated by the snubber network and capacitive load described by open-loop equation (17). The total phase shift of the compensated buffer at unity gain is increased from −225° to −134.5°; therefore, the circuit with a 45.5° phase margin is stabilized.

As the conditions of inequalities (14) and (16) are relaxed, poles p_1 and p_2 tend to converge toward the zero at ω_0 and the wide dome-shaped region of minimum phase, as seen in figure 6, shrinks in both width and height. Parametric studies verified that as R_A increases while maintaining a constant $C_A R_A$ product, pole p_2 approaches the zero at ω_0. In the limit this results in zero-pole cancellation with only a single pole remaining without corrective phase lead or the ability to suppress oscillation. Note also that the final values of resistor R_A and capacitor C_A are surprisingly low and high, respectively.

Uncompensated Filter Output Circuit

The open-loop transfer function of the uncompensated filter output circuit shown in figure 2, without the snubber network, including the equivalent operational amplifier transfer function, open-loop gain K, open-loop source resistance R_S, gain and noise roll-off network $R_F C_F R_1$, and load capacitance C_L, is found by circuit analysis to be given by

$$T_U(s) = \frac{E_o(s)}{E_i(s)} = \frac{KR_1(1+\tau_F s)}{(1+\tau_1 s)(1+\tau_2 s)(c_0 + c_1 s + c_2 s^2)} \quad (18)$$

where

$$\tau_1 = 1/(20\pi)$$

$$\tau_2 = 1/(10^7\pi)$$

$$\tau_F = R_F C_F$$

$$c_0 = R_1 + R_S + R_F$$

$$c_1 = (R_1 + R_F) R_S C_L + (R_S + R_1) R_F C_F$$

$$c_2 = C_A R_S R_1 R_F C_F$$

The gain-phase plot of the transfer function of equation (18), presented in figure 8, indicates that the closed-loop system is unstable with a phase margin of −10.5°.

Compensated Filter Output Circuit

Compensation of the filter output circuit using the snubber network is analogous to that of the unity-gain buffer. The open-loop transfer function of the compensated filter circuit shown in figure 2, including the equivalent operational amplifier transfer function, open-loop source resistance R_S, gain K, snubber network $R_A C_A$, gain and noise roll-off network $R_F C_F R_1$, and load capacitance C_L is found to be given as follows:

$$T(s) = \frac{E_o(s)}{E_i(s)} = \frac{KR_1(1+\tau_F s)(1+\tau_A s)}{(1+\tau_1 s)(1+\tau_2 s)(a_0 + a_1 s + a_2 s^2 + a_3 s^3)} \quad (19)$$

where

$$a_0 = R_1 + R_S + R_F$$

$$a_1 = (R_1 R_A + R_1 R_S + R_F R_A + R_F R_S + R_S R_A) C_A + (R_1 + R_F) R_S C_L + (R_S + R_1) R_F C_F$$

$$a_2 = (R_1 + R_F) R_S R_A C_L C_A + (R_1 + R_S) R_A R_F C_F C_A + (C_L + C_A) R_S R_1 R_F C_F$$

$$a_3 = R_1 R_F R_A R_S C_F C_L C_A$$

As seen in the gain-phase plot of equation (19) shown in figure 9, installing the snubber circuit into the filter output circuit, using component values of R_A = 1 Ω and C_A = 220 nF obtained as before reduces the overall open-loop gain in the formerly unstable region (10^7 rad/sec) by approximately 6 dB and increases the phase shift by 56°. Thus, the phase margin is increased sufficiently to 45° to stabilize the circuit.

Closed-Loop Response of Compensated Filter

The closed-loop gain frequency response appears in figure 10 for the values of C_A = 220 nF and

$R_A = 1\ \Omega$. For comparison the figure also illustrates the case for $C_A = 1.0\ \mu F$ and $R_A = 1\ \Omega$. Note that although the two responses are similar, the former case furnishes slightly faster response as predicted by its 45° phase margin.

Results

After installation of the snubber circuit into the AOA signal conditioning package, laboratory calibration tests indicate the following performance:

1. Stable operation with capacitive loads up to 1 μF
2. 10-μV DC offset
3. 13-μV rms noise from 0 to 3 kHz

The computed DC output impedance is 60 μΩ, and the computed gain accuracy is 0.007 percent based on the use of 0.005 percent gain resistor tolerances. The additional gain error with 10 kΩ DAS input impedance is less than 1 ppm, whereas with 50 Ω DC output impedance the gain error with 10 kΩ DAS input impedance would be 0.5 percent. The common mode rejection ratio of the 2652A operational amplifier is greater than 120 dB. Thus, the design performance criteria are satisfied. High quality polypropylene capacitors are employed for stability and low dielectric absorption properties to ensure adequate charge and discharge rates at microvolt voltage levels for AOA data acquisition.

Concluding Remarks

Practical design formulas have been developed to obtain initial approximate component values for the snubber circuit, given the open-loop output resistance of the operational amplifier, the load capacitance, and the frequency of regenerative oscillation. Parametric studies using gain-phase analysis are useful to trim the initial predicted component values to final values providing prescribed performance and phase margin criteria. A number of control system design software packages are available with which gain-phase graphical analysis can be conveniently performed. This technique is applicable to any precision amplifier circuitry to suppress regenerative oscillation due to output cable capacitive loading.

NASA Langley Research Center
Hampton, VA 23681-0001
March 16, 1995

References

1. Finley, Tom D.; and Tcheng, Ping: Model Attitude Measurements at NASA Langley Research Center. AIAA-92-0763, Jan. 1992.
2. Anon.: *Burr-Brown Integrated Circuits Data Book Supplement*, Volume 33b. Burr-Brown Corp., 1990, p. 2-53.
3. Anon.: *Linear Databook*. 400041, Rev. 1, Natl. Semiconductor Corp., 1988.
4. Anon.: *Reference Data for Radio Engineers*. 6th Edition, Howard W. Sams & Co., 1981, p. 10-3.
5. Anon.: *Linear Circuits Data Book 1992*. Texas Instrum., 1992.
6. Melsa, James L.; and Schultz, Donald G.: *Linear Control Systems*. McGraw-Hill Book Co., 1969.
7. Storer, James E.: *Passive Network Synthesis*. McGraw-Hill Book Co., 1957.

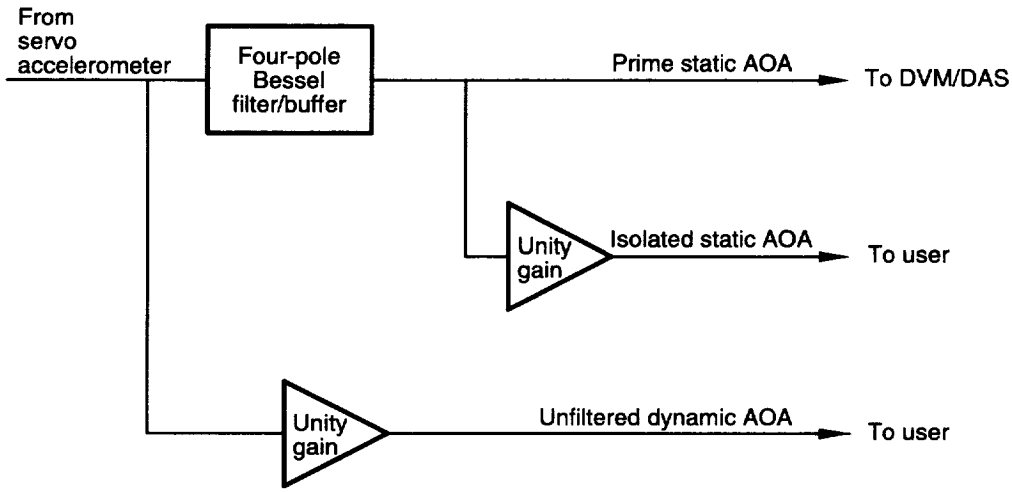

Figure 1. Block diagram of AOA signal conditioner.

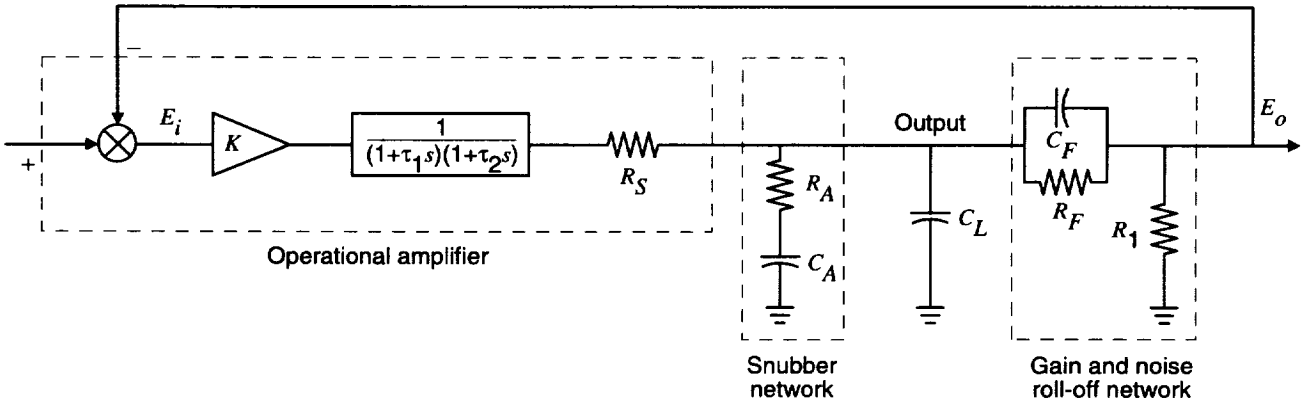

Figure 2. Output stage of active filter.

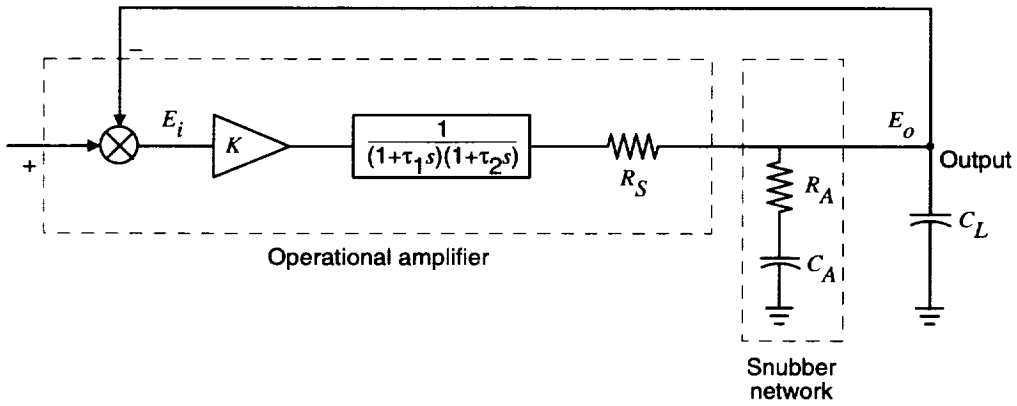

Figure 3. Unity-gain buffer.

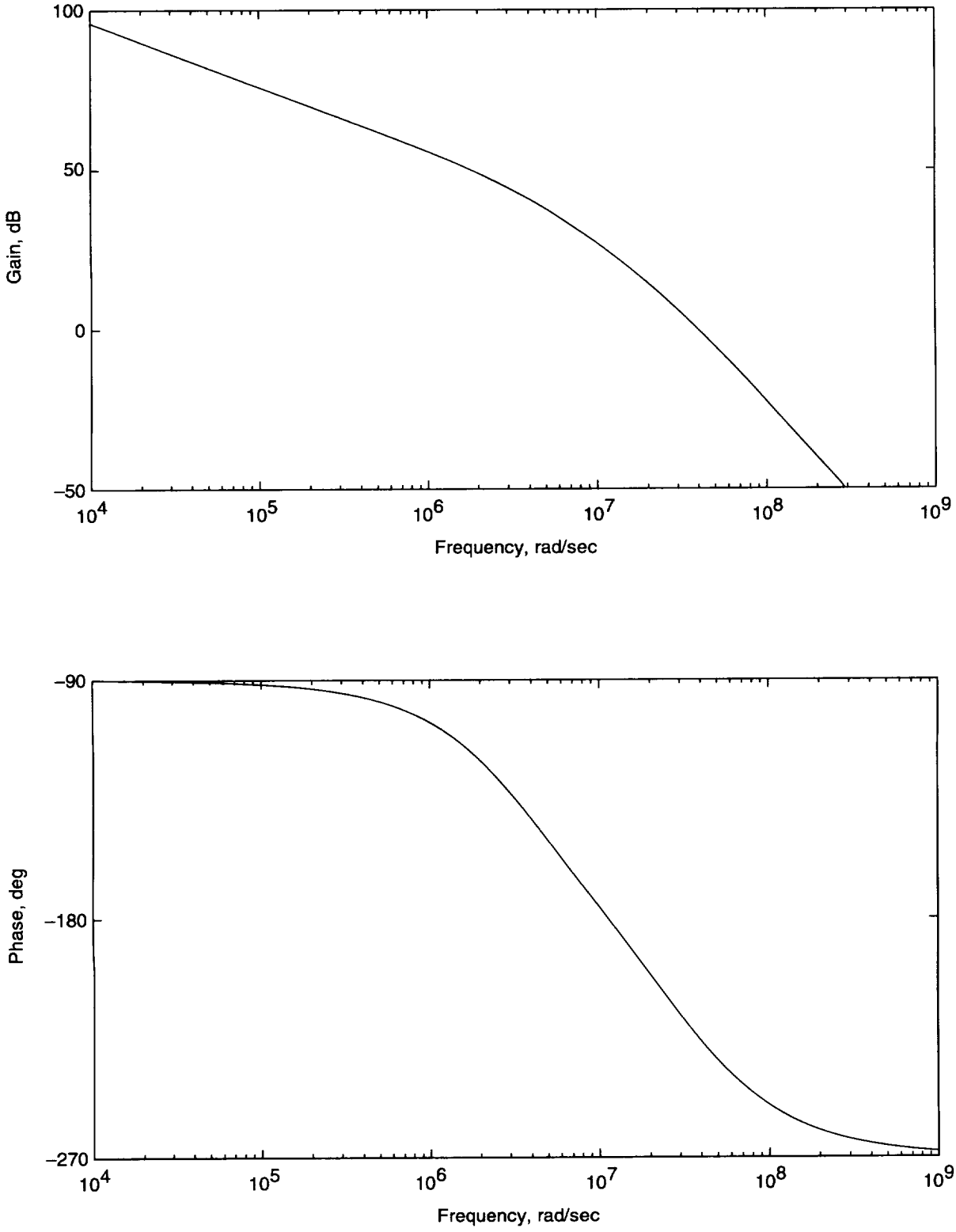

Figure 4. Gain-phase plot of unity-gain buffer. C_L = 5 nF.

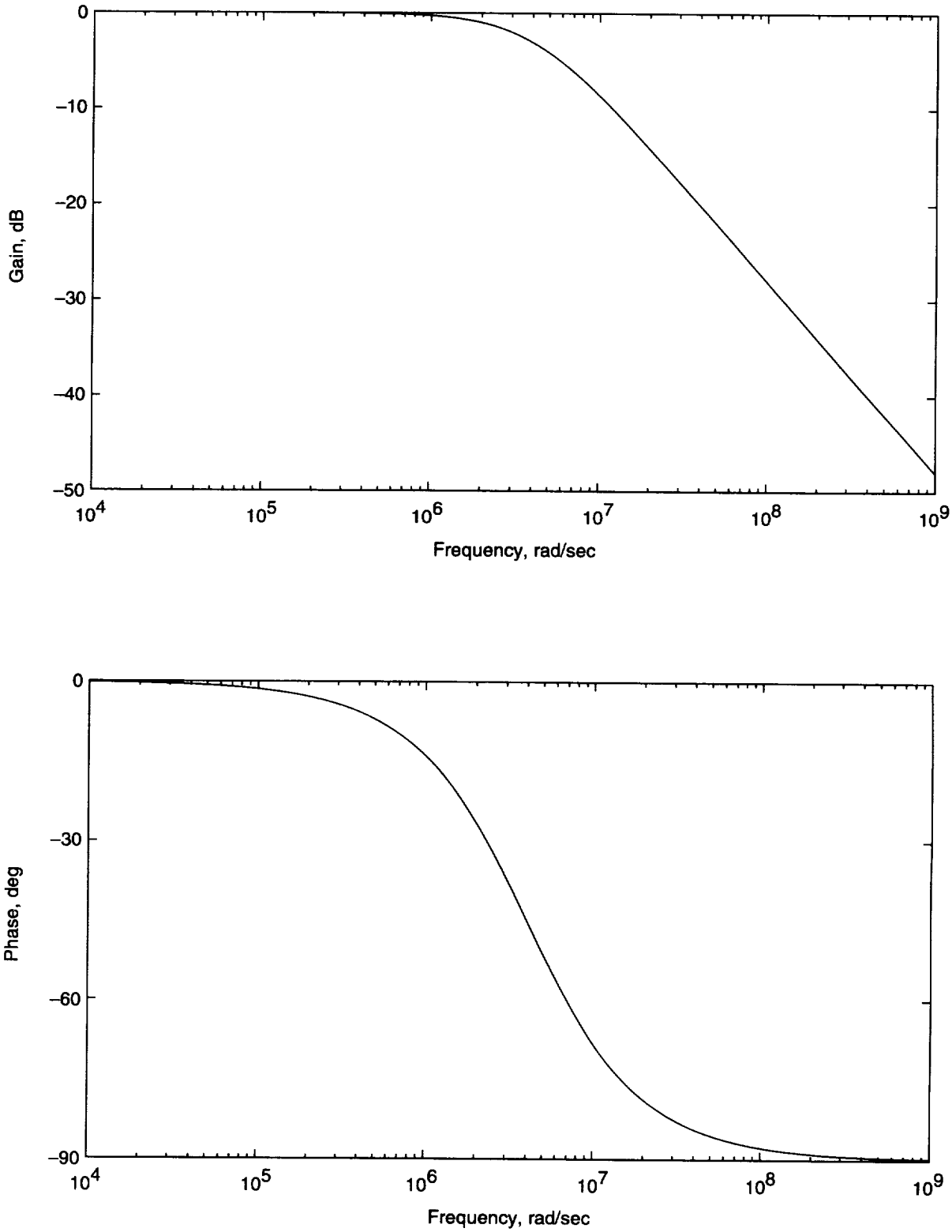

Figure 5. Gain-phase plot of load circuit. C_L = 5 nF.

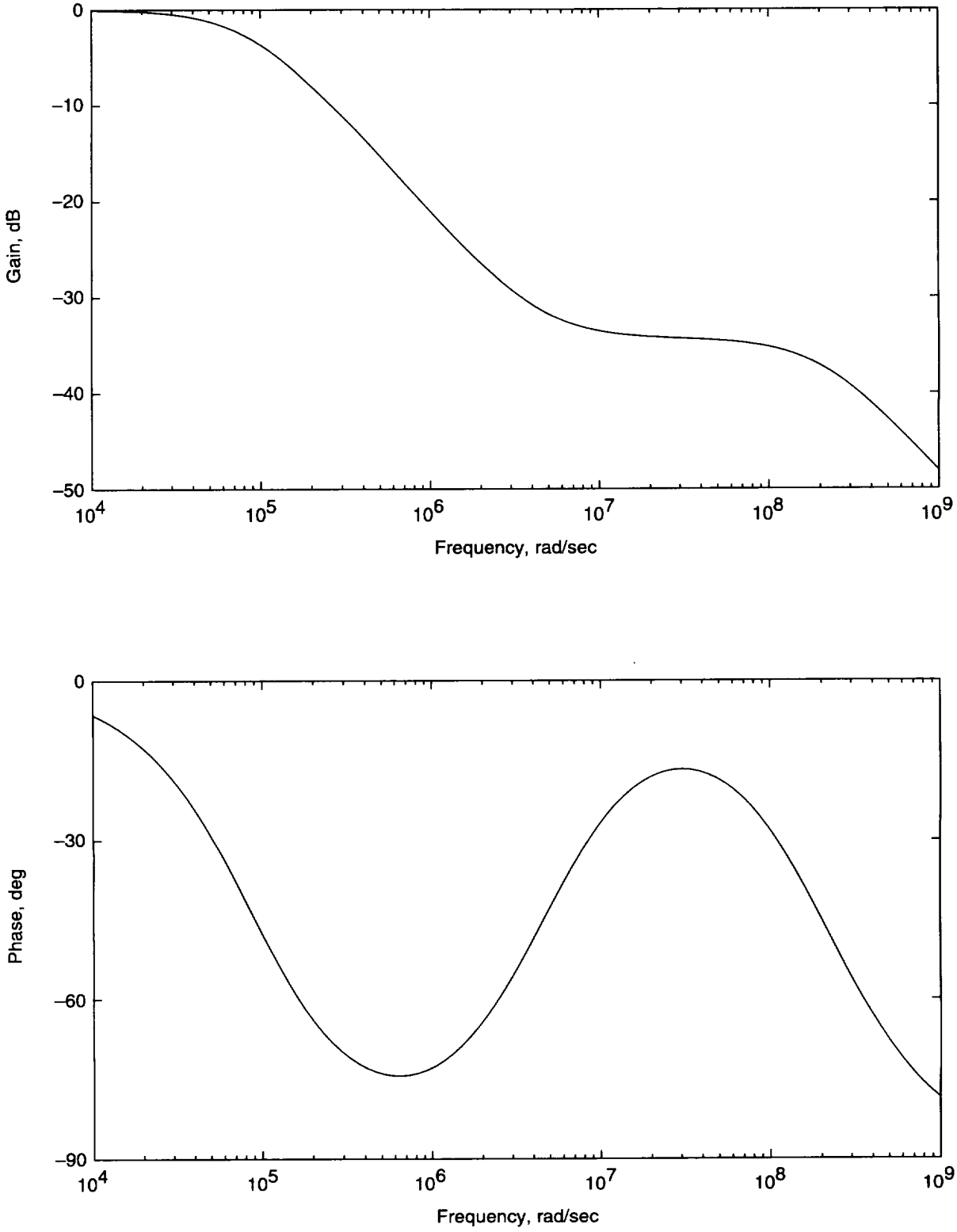

Figure 6. Gain-phase plot of load circuit with snubber. C_L = 5 nF; C_A = 220 nF; R_A = 1Ω.

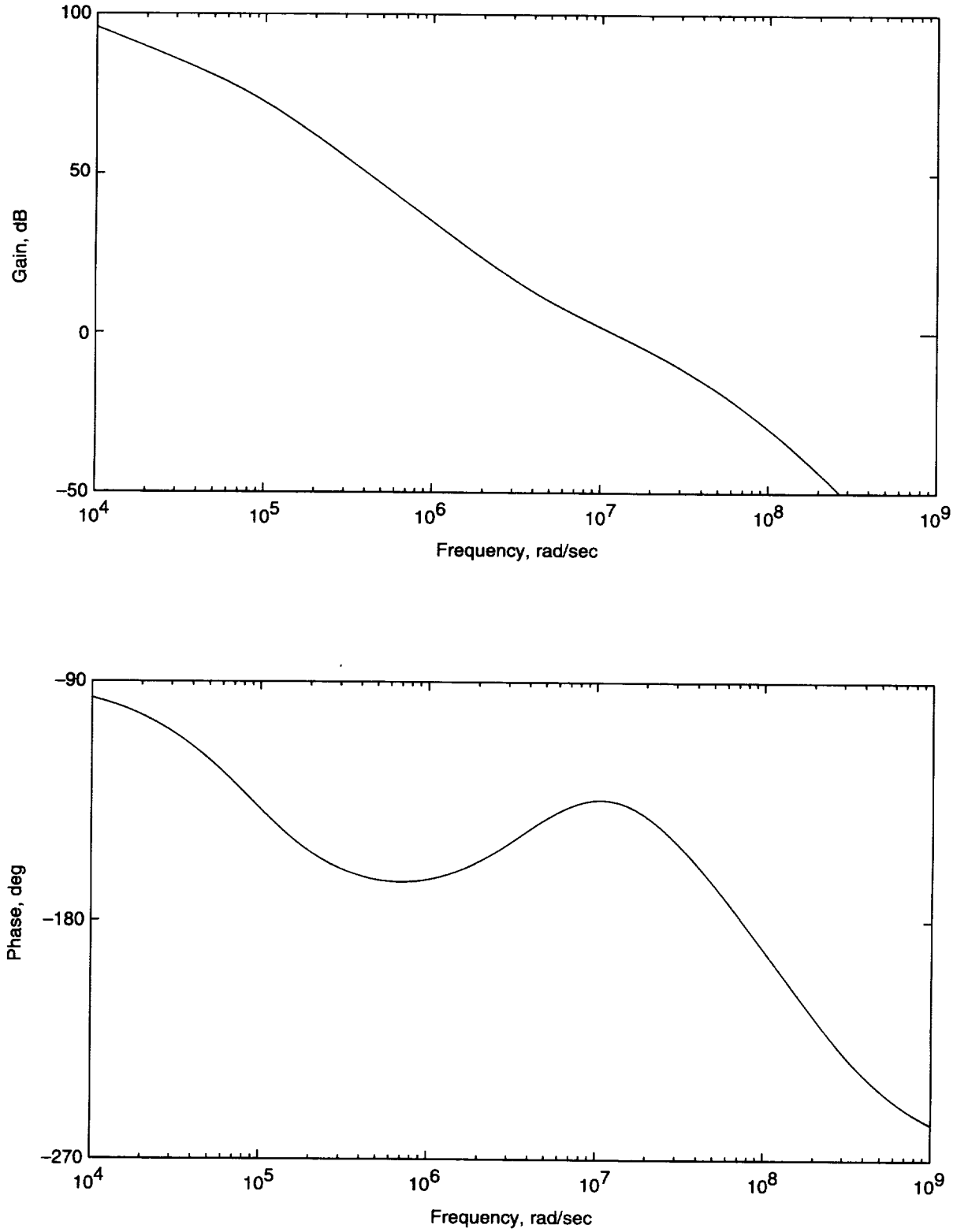

Figure 7. Gain-phase plot of compensated unity-gain buffer. $R_A = 1\ \Omega$; $C_A = 220$ nF; $C_L = 5$ nF.

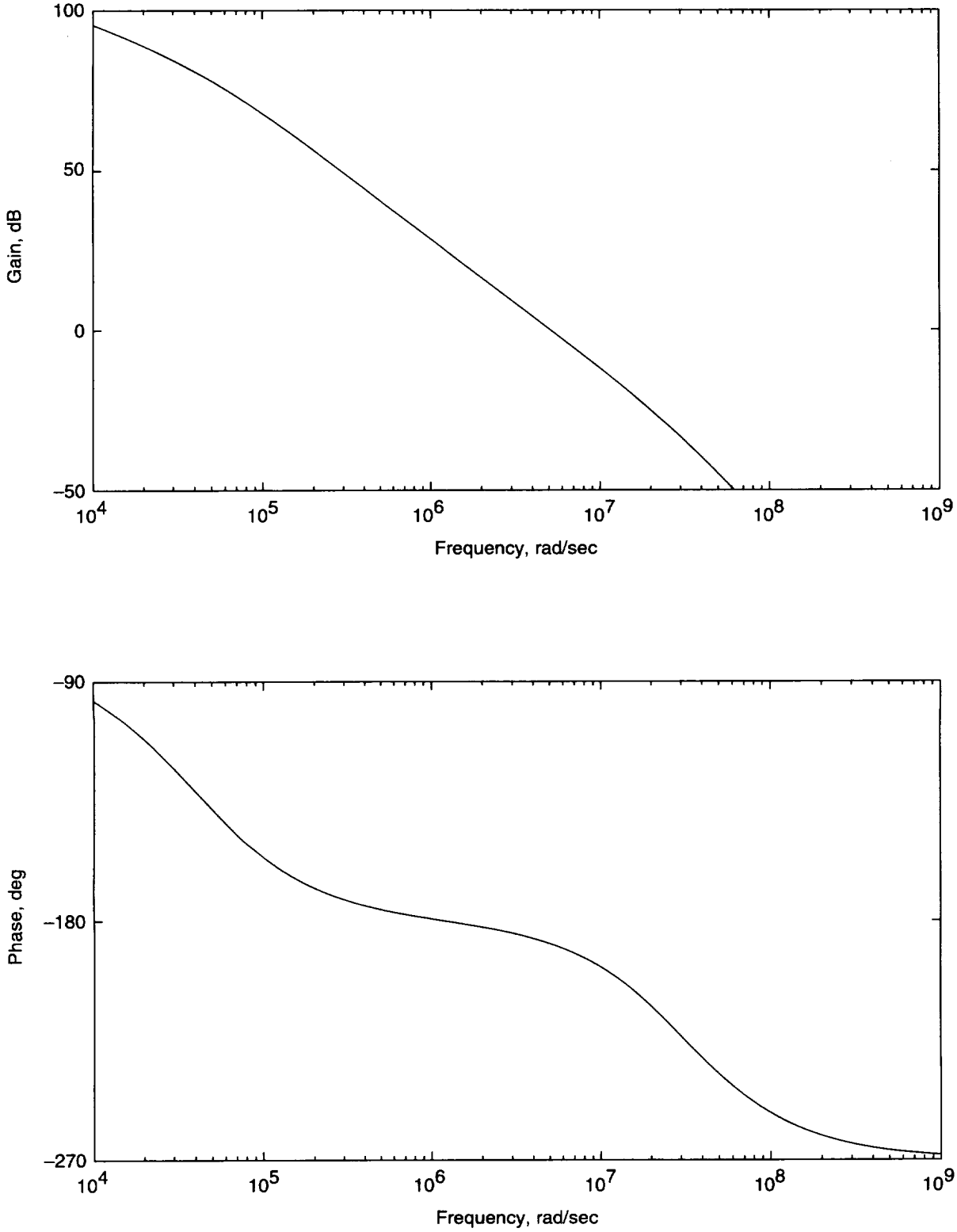

Figure 8. Gain-phase plot of uncompensated filter with noise roll-off and load. C_L = 5 nF.

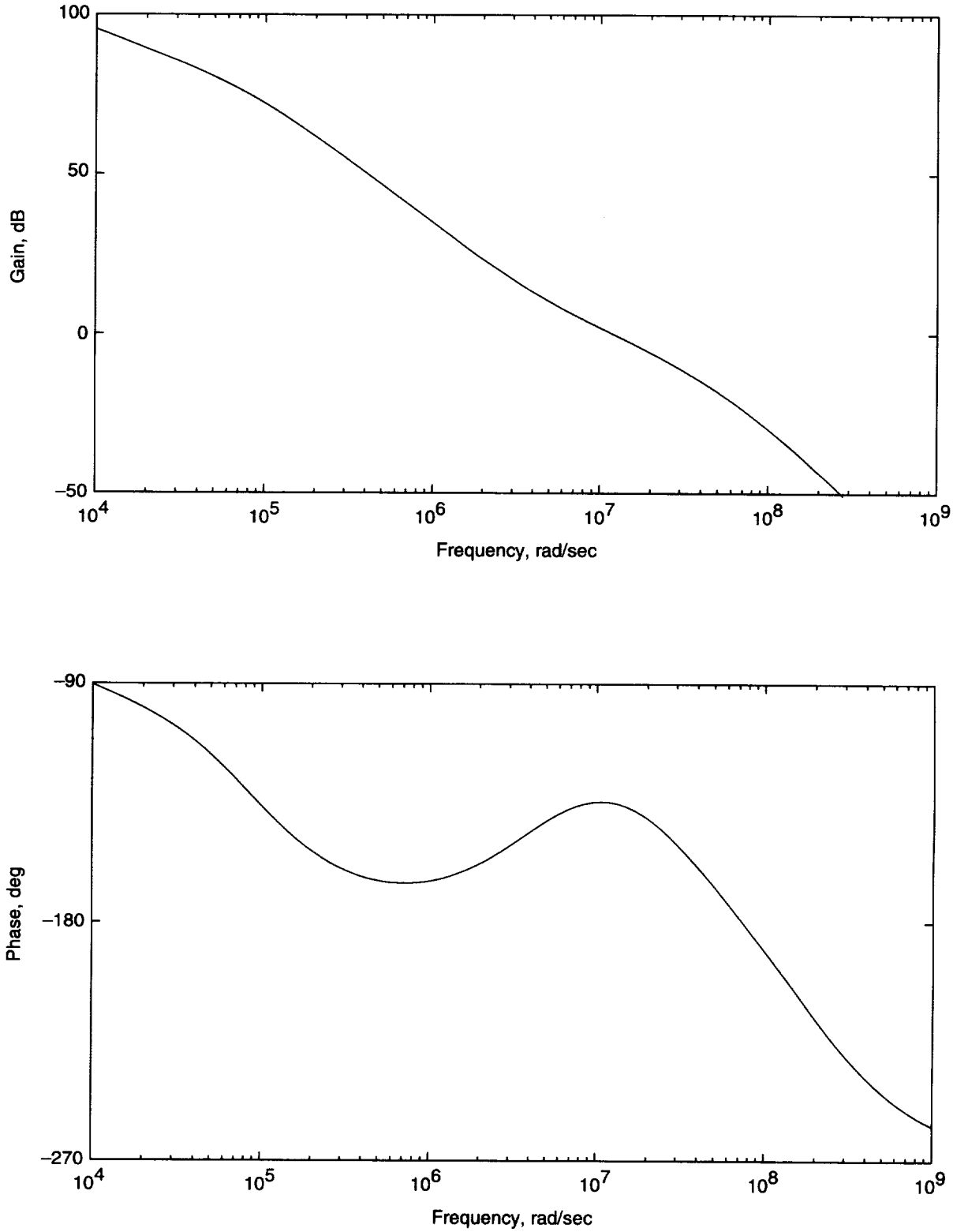

Figure 9. Gain-phase plot of compensated filter. $R_A = 1\ \Omega$; $C_A = 220$ nF; $C_L = 5$ nF.

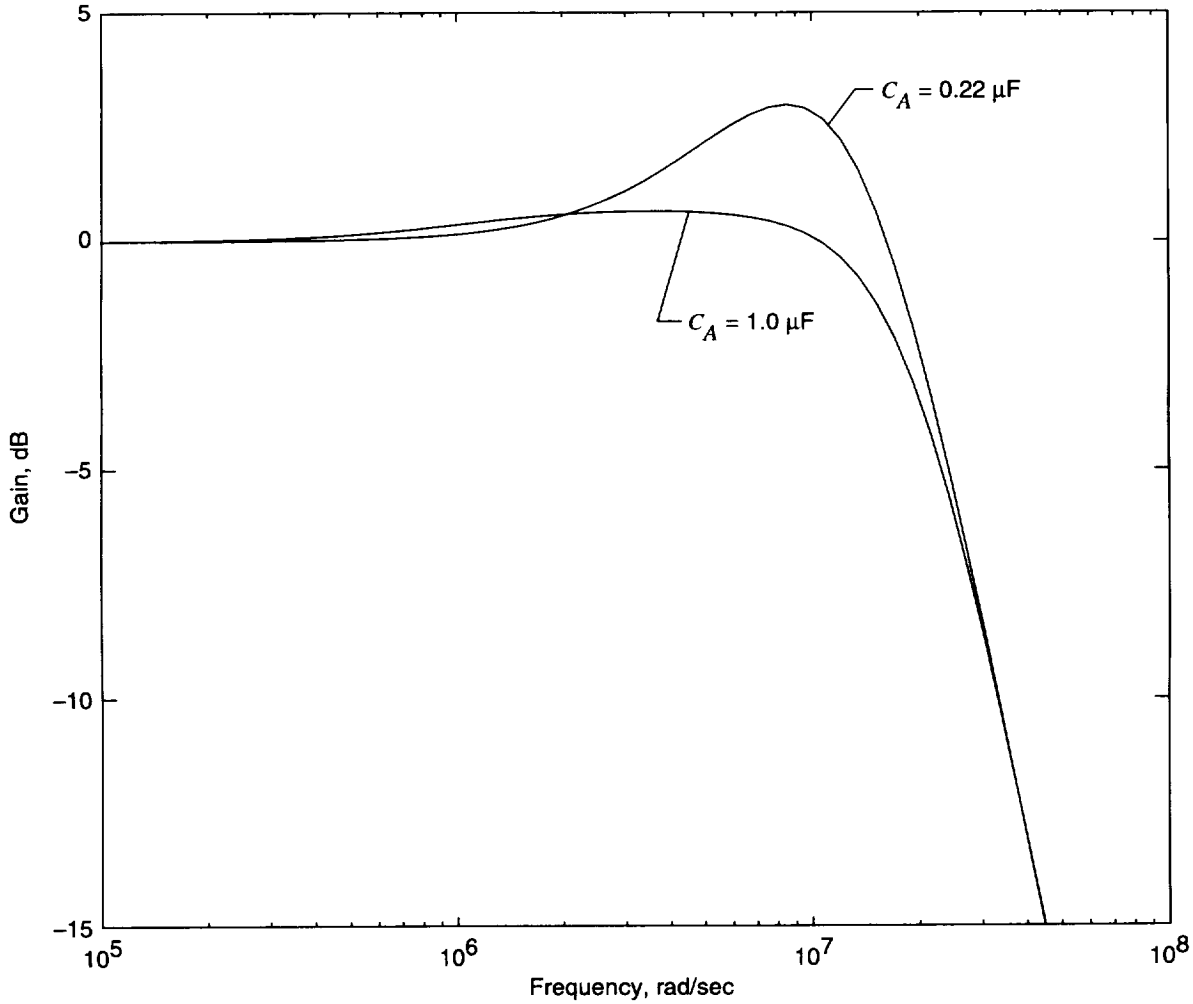

Figure 10. Closed-loop frequency response of compensated filter.

REPORT DOCUMENTATION PAGE

Form Approved
OMB No. 0704-0188

1. AGENCY USE ONLY *(Leave blank)*	2. REPORT DATE	3. REPORT TYPE AND DATES COVERED
	May 1995	Technical Memorandum

4. TITLE AND SUBTITLE
High-Precision Buffer Circuit for Suppression of Regenerative Oscillation

5. FUNDING NUMBERS
WU 505-59-54-02

6. AUTHOR(S)
John S. Tripp, David A. Hare, and Ping Tcheng

7. PERFORMING ORGANZATION NAME(S) AND ADDRESS(ES)
NASA Langley Research Center
Hampton, VA 23681-0001

8. PERFORMING ORGANIZATION REPORT NUMBER
L-17453

9. SPONSORIING/MONITORING AGENCY NAME(S) AND ADDRESS(ES)
National Aeronautics and Space Administration
Washington, DC 20546-0001

10. SPONSORING/MONITORING AGENCY REPORT NUMBER
NASA TM-4658

11. SUPPLEMENTARY NOTES

12a. DISTRIBUTION/AVAILABILITY STATEMENT
Unclassified–Unlimited
Subject Category 35
Availability: NASA CASI (301) 621-0390

12b. DISTRIBUTION CODE

13. ABSTRACT *(Maximum 200 words)*
Precision analog signal conditioning electronics have been developed for wind tunnel model attitude inertial sensors. This application requires low-noise, stable, microvolt-level DC performance and a high-precision buffered output. Capacitive loading of the operational amplifier output stages due to the wind tunnel analog signal distribution facilities caused regenerative oscillation and consequent rectification bias errors. Oscillation suppression techniques commonly used in audio applications were inadequate to maintain the performance requirements for the measurement of attitude for wind tunnel models. Feedback control theory is applied to develop a suppression technique based on a known compensation (snubber) circuit, which provides superior oscillation suppression with high output isolation and preserves the low-noise low-offset performance of the signal conditioning electronics. A practical design technique is developed to select the parameters for the compensation circuit to suppress regenerative oscillation occurring when typical shielded cable loads are driven.

14. SUBJECT TERMS
Regenerative oscillation; Oscillation suppression; Precision amplifier; Compensation circuit; Snubber circuit; Buffer circuit; Capacitive loading

15. NUMBER OF PAGES
16

16. PRICE CODE
A03

17. SECURITY CLASSIFICATION OF REPORT	18. SECURITY CLASSIFICATION OF THIS PAGE	19. SECURITY CLASSIFICATION OF ABSTRACT	20. LIMITATION OF ABSTRACT
Unclassified	Unclassified	Unclassified	